frontiers | Frontiers in Energy Research

BRIEF RESEARCH REPORT
published: 24 June 2022
doi: 10.3389/fenrg.2022.879257

The Flexible and Transparent Film Heaters Based on Regenerated Cellulose and Carbon Nanotubes

*Jiedong Cui[1], Pengbo Lu[1,2], Yinghui Li[1], Ke Xu[1], Yang Li[1], Haoyu Shen[1], Chaocheng Liu[1], Tianyi Zhang[2] and Detao Liu[1]**

[1]School of Light Industry and Engineering, South China University of Technology, Guangzhou, China, [2]Gree Intelligent Equipment Co., Ltd., Zhuhai, China

The flexible and transparent film heaters (FTFHs) with the advantages of mechanical flexibility, portability, and excellent electrothermal performance, are key to the next generation portable, wearable heaters and thermal protection systems. However, the present flexible and transparent substrates of FTFHs are fabricated by typical plastic PET films, which suffer from poor interfacial adhesion with the thermally conductive materials. In this work, the transparent regenerated cellulose fibers made of completely dissolved in NMMO solution followed by regeneration process is presented to disperse and support carbon nanotubes (CNTs) by a vacuum-dewatering process. In the presence of cellulose fibers, these CNTs have strong hydrogen bonding properties in the dehydration-deposition process and thus respond to tight intertwining structures in fibrous composites. The resulting regenerated cellulose fibers exhibit high optical transparency of 88% (@550 nm) and good mechanical properties (30 MPa). Interestingly, the FTFHs show a rapid heating response, high generation temperature, and resistance stability for up to 2 h. The FTFHs made with earth-abundant, cost-effective, and recyclable materials, have excellent potential in the areas of green flexible and transparent film heaters.

Keywords: flexible heaters, regenerated cellulose, NMMO, CNFS, transparency

OPEN ACCESS

Edited by:
Xiaojun Shen,
Dalian Institute of Chemical Physics, (CAS), China

Reviewed by:
Li Fengfeng,
Qilu University of Technology, China
Liangcai Peng,
Huazhong Agricultural University, China

****Correspondence:***
Detao Liu
dtliu@scut.edu.cn

Specialty section:
This article was submitted to Bioenergy and Biofuels, a section of the journal Frontiers in Energy Research

Received: *19 February 2022*
Accepted: *30 May 2022*
Published: *24 June 2022*

Citation:
Cui J, Lu P, Li Y, Xu K, Li Y, Shen H, Liu C, Zhang T and Liu D (2022) The Flexible and Transparent Film Heaters Based on Regenerated Cellulose and Carbon Nanotubes. Front. Energy Res. 10:879257. doi: 10.3389/fenrg.2022.879257

INTRODUCTION

Due to its attractive characteristics of portability, quick response, and flexibility, the flexible and transparent film heaters (FTFHs) are directing the development of the next generation of flexible heaters such as vehicle window defrosters, outdoor panel displays, and automobile mirrors (Madaria et al., 2011; Lee et al., 2016; Song et al., 2017; Lee et al., 2020b), and so on. Until now, the FTFHs are typically fabricated by sputtering, coating, or printing electrothermal materials such as ITO (De et al., 2009), graphene (Zhang Q. et al., 2017), conducting polymers (Kim et al., 2011) and AgNWs (Wang et al., 2018) onto the surface of flexible polyethylene terephthalate (PET) (Tokuno et al., 2011) or rigid glass substrates. However, research efforts over the past years have encountered numerous problems, such as non-biodegradability, fragility, and non-transparency with low electrothermal efficiency (Jang and Choi, 2021; Yu et al., 2021). More importantly, loading electrothermal materials onto the smooth-faced PET, glass, or metal substrates, renders the poor adhesion and easier debonding between them (Hutchinson and Suo, 1992; Yu et al., 2019). Compared to the typical substrates with mechanical brittleness, scarcity, and fragile property (Cotterell and Chen, 2004), the flexibly porous fiber substrates display outstanding binding force due to their abundant hydroxyl groups combined with electrothermal materials. Furthermore, with porosity present, this FTFHs

composite is usually opaque, and hence a general mechanism to decrease the contradiction between them remains intricate.

Nowadays, natural biopolymers have been utilized to substitute plastic-based film substrates. Cellulose, an inexhaustible biopolymer resource, has excellent biocompatibility, biodegradability, mechanical and thermal stabilities (De France et al., 2020; Ma et al., 2021). Cellulose is an ideal candidate material to replace PET film substrates due to the rich hydrogen groups between cellulose molecules that can promote fiber bonding and improve the mechanical strength of the films (Ji et al., 2021). However, regular films made of cellulose fibers have high surface roughness and porosity, the natural difference in refractive index between air and cellulose make a negative influence on the transparency of substrate materials and electrical properties of devices (Fang et al., 2014). Su et al. (Su et al., 2019) fabricated FTFHs using a solution-based pressured extrusion papermaking process that conducting polymer (PEDOT: PSS) enhanced silver nanowire (AgNW) networks adsorbed on the cellulose nanofibers (CNFs) film substrate. CNFs are outstanding materials to prepare transparent films because there are few void spaces inside the paper, and the refractive index of light is reduced (Isogai et al., 2011; Isogai, 2013). However, the preparation process of CNFs is complicated and has high energy consumption, time consumption, and high cost, limiting the large-scale production of flexible and transparent film substrates (Li et al., 2019). Therefore, it is of significance to look for novel alternative materials to prepare FTFHs with good electrical conductivity, excellent mechanical properties, flexibility, and environmental friendliness. Interestingly, direct dissolution of cellulose with cellulose solvents assisted by subsequent treatment is an efficient process to produce transparent films on a large scale and at a low cost. Recent studies have shown that ionic liquids are suitable solvents for cellulose, which can dissolve cellulose and then regenerate it in an aqueous solution or ethanol solution to prepare regenerated cellulose. And regenerated cellulose is also an excellent material to fabricate transparent film substrates. (Lu et al., 2017a) firstly reported an all-cellulose transparent film fabricated by a novel microwave-assisted ionic liquids technology, which shows high optical transparency of 82% (@550 nm) and high tensile stress (46.0 MPa). The most common solvents used in these processes mainly include NaOH/urea aqueous solutions (Kong et al., 2021), LiCl/DMAc (Gao et al., 2021), PF/DMSO (He and Wang, 2000), and N-methyl Morpholine, Nmethylmorpholine-N-oxide (NMMO) (Protz et al., 2021). Among them, NMMO has attracted significant attention because of its green, non-toxic, high recyclability (99%), and good solubility (Zhang Y. et al., 2017). In addition, Carbon nanotubes (CNTs) (Zhang et al., 2006; Cao and Rogers, 2009) have the advantages of outstanding thermal conductivity, excellent mechanical flexibility, and exceptional optical properties, which are regarded as the ideal candidates for replacing ITO. CNTs can also be cross-linked with cellulose by hydrogen bonding, which solves poor adhesion between conductive materials and the transparent substrates.

In this work, we fabricated FTFHs with high optical transparency and promising electrothermal properties by using regenerated cellulose to prepare film as flexible transparent substrates and CNTs as thermally conductive materials. This new method for preparing FTFHs had the following advantages: 1) The NMMO solution is non-toxic, recyclable and high-efficiency in dissolving cellulose; 2) Regenerated cellulose is an outstanding material for preparing flexible and transparent films that can substitute PET films for better bonding with thermal conductive materials; 3) The FTFHs made of regenerated cellulose and CNFs, exhibits high generation temperature (50.5°C), shorter response time (15 s) and long-term stability of resistance (2 h), shows a good case for designing FTFHs with high-performance and environmental friendliness in flexible heaters applications.

EXPERIMENTAL

Materials

Commercial eucalyptus dissolving pulp was used as the raw cellulose source material and was purchased from Guangzhou Chenhui Paper Co., Ltd. (China) and the average polymerization degree of eucalyptus dissolving pulp was 652. The carbon nanotubes (~50 μm) were purchased from Shanghai Lishuo Co., Ltd. (China); N-methyl -morpholine-N-oxide (NMMO) was purchased from Aladdin-Reagent Co., Ltd. (Shanghai China). All the reagents were used as received.

Preparation of Regenerated Cellulose

Firstly, the mass fraction of 50% NMMO solution purchased directly was diluted to obtain an aqueous NMMO solution with a mass fraction of 13%. Then 2 g cellulose fibers were added to the 100 ml 13% aqueous NMMO solution and stirred for 2 h at 90°C to obtain the dissolved cellulose. Add dissolved cellulose solution to deionized water and rotate it in a high-speed emulsifier at 5000 rpm/min to get the regenerated cellulose. The regenerated cellulose with a concentration of 0.5 wt%% was centrifuged at 4000 rpm/min for 10 min and the supernatant was smaller than regenerated cellulose and the turbid solution was larger than regenerated cellulose.

Dispersion of Carbon Nanotubes

The CNTs used in this study are multiwalled CNTs synthesized by chemical vapor deposition and the length of the CNTs is about 50 μm. First, 40 ml HNO_3 and 120 ml H_2SO_4 were added into the beaker to mix evenly, and 0.4 g CNTs were added to the mixed solution. After ultrasonic treatment for 2 h, CNTs were centrifuged at 4000 rpm/min for 20 min, and then the CNTs were washed to neutral with deionized water. Then a 0.5% CNT dispersion was prepared with deionized water.

Fabrication of Flexible and Transparent Film Heaters

The flexible transparent paper with a base density of 30 g/m^2 and an area of 28 cm^2 was prepared by suction filtration. Then, the dispersed CNTs solution was poured on the surface of the flexible transparent paper and continued to filter. After carbon nanotubes

were completely deposited on transparent paper, FTFHs were obtained by hot pressing at 110°C and 0.4 MPa for 5 min. For comparison, we also prepared transparent films using the smaller regenerated cellulose (supernatant of the solution)as raw material without CNTs, called Film-1 and using the larger regenerated (raw solution) cellulose as raw material without CNTs, called Film-2. The FTFHs with contents of CNTs were 0.1 g/m^2, 0.15 g/m^2 and 0.2 g/m^2 were called FTFH-0.1, FTFH-0.15, FTFH-0.2.

Characterizations

Scanning Electron Microscopy

The film morphologies were tested with scanning electron microscopy (SEM) with an accelerating voltage at 5–10 kV. A KajaaniFS300 Fiber Analyzer was used to quantitatively analyze the dimensions of the regenerated cellulose fibers and the original cellulose fibers in DI water (18.2 MΩ/cm).

Transmission Electron Microscopy

The samples were observed with transmission electron microscopy (TEM) using a JEM-2100 transmission electron microscope at an accelerator voltage of 200 kV. A droplet of the diluted slurry was dropped on the carbon-coated electron microscopy grid and then negatively stained with 1 wt% phosphotungstic acid solution to enhance image contrast. The dimensions of the DCCs were determined from the TEM images using the Image J TEM-image-processing software.

Transmittance

UV-Vis spectrometer with an integrating sphere (UV-9000 Shanghai Yuanyi Inc. China) was used to measure the total transmittance of the films in a wavelength range of 400–900 nm.

X-ray Diffraction

X-ray diffraction (XRD) patterns of the film samples were carried out on an X-ray diffractometer (D8 ADVANCE, Bruker Inc., Germany) with area detector operating at a voltage of 40 kV and a current of 40 mA using Cu Kα radiation (λ= 0.154 nm). The scanning scope of 2θ was from 4° to 50° at room temperature.

Thermogravimetric Analysis

Thermal stability and changes in degradation patterns associated with regenerated cellulose film and original cellulose were assessed with TGA (TA Instruments TGA Q500). Samples were tested under a flowing nitrogen atmosphere with sample 5–7 mg. Samples were heated from room temperature to 120°C at a rate of 10°C/min under a flowing nitrogen atmosphere, then held at 120°C for 20 min, and then heated to 600°C at a rate of 10°C/min.

Mechanical Strength

The mechanical strength of samples was measured using a universal tensile tester (Instron5565, Instron Instruments Inc. United States). Samples were cut into 5.0 mm × 25.0 mm. The resistances of the FTFHs were recorded by a multimeter (VC890D, China). Samples were cut into 25.0 mm × 25.0 mm. The samples were placed in a constant temperature and humidity chamber at (50 ± 1) % relative humidity (RH) and (23 ± 1)°C for 24 h to ensure the stabilization of their water content before characterization.

Temperatures and Heat Distributions

The temperatures and heat distributions of the FTFHs were measured using a thermal imager (DT-980, China). Samples were cut into 80.0 mm × 80.0 mm. The applied DC voltage was supplied by a power supply (HY3005ET, China). Two copper conductive tapes were pasted at the FTFHs to form a complete circuit system.

RESULTS AND DISCUSSION

Fabrication Process for the Flexible and Transparent Film Heaters

The schematic illustration of the procedure of FTFHs was shown in **Figure 1**. Ordinary paper made of cellulose is optically opaque, due to the void spaces in the fiber network and scattering of light at the interfacial area between the fibers, hindering their practical application as substrates in transparent film heaters. The transparent film made of regenerated cellulose reported in this work exhibited excellent optical transparency. The original cellulose dissolves in the mass fraction of 13% aqueous NMMO solution then regenerated in deionized water. NMMO is a tertiary aliphatic amine N-oxide hydrate with strong dipole N-O moiety. The oxygen groups form one or two hydrogen bonds with an anhydrous glucopyranose unit (AGU) of cellulose, which leads to the cleavage of intermolecular hydrogen bonds of cellulose chains and cellulose is dissolved. The dissolved cellulose was added to deionized water, and the N-O groups of NMMO form hydrogen bonds with the hydroxyl groups of water molecules (Bang et al., 1999; Zimmermann et al., 2016; Sayyed et al., 2019). The regenerated cellulose is obtained due to the released cellulose molecules rapidly regenerate by reforming new hydrogen-bond networks. CNTs were tightly deposited on the flexible transparent film by suction filtration. The oxidized CNTs have hydroxyl and carboxyl groups on the surface (Guo et al., 2018), which form hydrogen bonding with regenerated cellulose. The compatibility and interaction between the CNTs and regenerated cellulose enhanced the interfacial adhesion. Through the hot-pressing process, the bonding strength between carbon nanotubes and regenerated cellulose is greatly improved, and the porosity of the film is reduced, which led to the increase in the mechanical strength and transparency of the film.

The Structure of Samples

The differences of Original paper (made of raw cellulose, by paper making), Film-1, and FTFHs have distinctly been observed from the scanning electron microscope (SEM) images by scanning cross-sections and fracture surfaces in **Figure 2**. As shown in **Figures 2A,B**, the surface of the original paper is rough and porous with long fibers attached intricately. The voids between the cellulose are the main reason for the opacity of papers (Khakalo et al., 2017). After dissolution and regeneration, the film prepared by regenerated cellulose has a smooth surface without apparent pores (**Figures 2C,D**). Accompanied by the

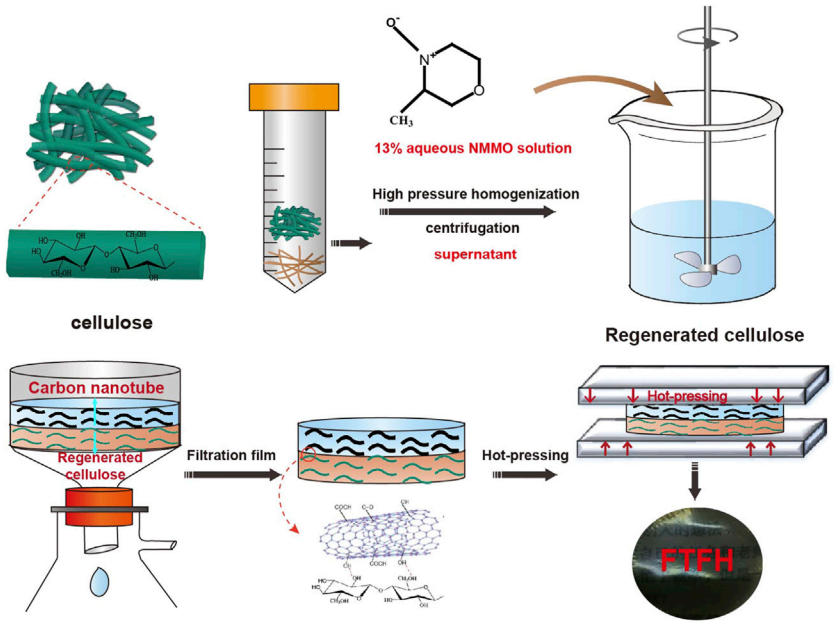

FIGURE 1 | Schematic illustration of the fabrication process for the FTFHs.

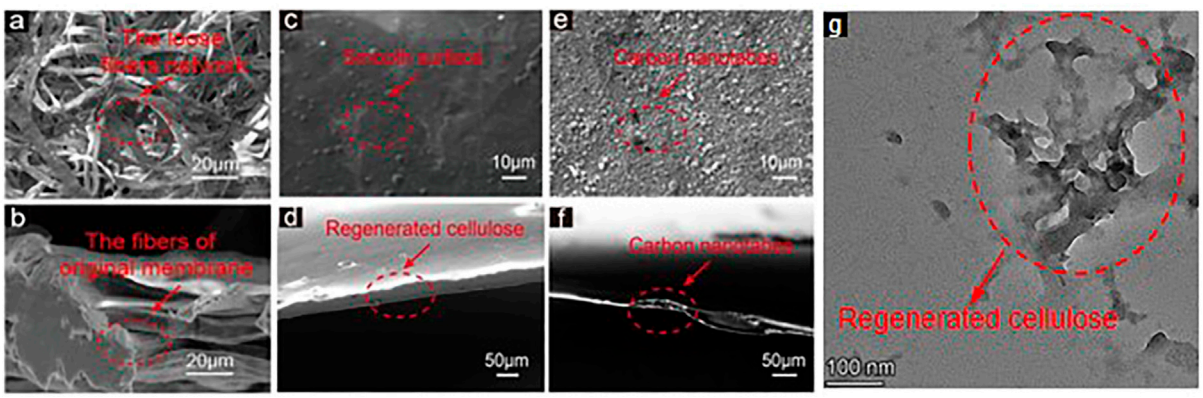

FIGURE 2 | SEM images of cross-sections: **(A)** Original paper; **(C)** Film-1; **(E)** FTFH; SEM images of the fracture surface: **(B)** Original paper; **(D)** Film-1; **(F)** FTFH; **(G)** TEM image of regenerated cellulose.

dissolution process, the hydrogen bond between the cellulose is destroyed and the cellulose is broken down into small sizes. The small size of cellulose is tightly intertwined due to hydrogen bonds during the filtration process, and the holes between the fibers are filled with smaller cellulose. CNTs are deposited onto the wet flexible transparent film to fabricate FTFHs. The surface of FTFHs in **Figure 2E** is significantly rougher than Film-1, due to the size of the CNTs is larger than the size of the underlying regenerated cellulose. The fracture surface of FTFHs in **Figure 2F** only shown the CNTs layer, and the cellulose fiber layer does not appear because it has not been sprayed with gold to prevent the effect of the metal gold coating on CNTs. As shown in **Figure 2G**, the length of regenerated cellulose is about 100–200 nm.

The dimension of cellulose fiber is an essential factor in affecting the transparency of the substrate. As shown in **Table 1**, the regenerated cellulose fibers have an average fiber length of 0.66 mm and an average fiber width of 11.45 μm, whereas original cellulose fibers have an average fiber length of 2.40 mm and an average fiber width of 25.82 μm. It is proved that the aqueous NMMO solvent can cleavage intermolecular hydrogen bonds of cellulose chains and reduce cellulose size, indicating that aqueous NMMO solvent is the excellent solvent system for cellulose. Regenerated cellulose fibers have a higher curl index (28.87%) but a lower kink index (9.63 L/m) compared to original pulp fibers, which is conducive to the formation of flexible transparent film. The fine content of the regenerated cellulose fibers (fiber length less than 200 mm, 66.98%) is much

TABLE 1 | Fiber dimension of regenerated cellulose and the original pulp fibers.

Samples	Length (mm)	Width (μm)	Curl index (%)	Kink index (L/m)	Cellulose fines (%)
Regenerated cellulose	0.66	11.45	28.87	9.36	66.98
Original cellulose	2.40	25.82	18.51	1334.82	8.33

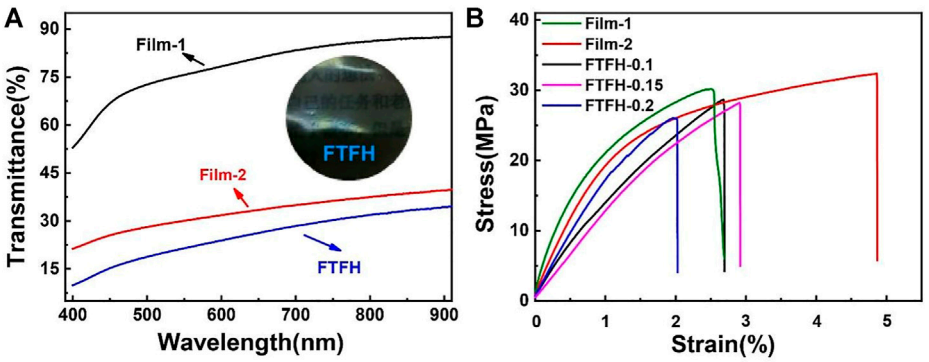

FIGURE 3 | (A) Optical transmittance plot for all Film-1, Film-2 and FTCT-0.15 in the range from 400–900 nm **(B)** Stress-strain curves of the Film-1, Film-2, FTFH-0.1, FTFH-0.15 and FTFH-0.2.

higher than that of original pulp fibers (8.33%). In the process of film formation, the rich hydroxyl among fines promotes the binding between the fibers, which reduces the void spaces of fines and improves the transparency of the film.

The Mechanical and Optical Performances of Samples

Transparency plays a crucial role for FTFHs, the transmittance of Film-1, Film-2, and FTFHs shown in **Figure 3A**. The Film-1 exhibits a high optical transmittance of 88% at the wavelength 550 nm, while the Film-2 is only 40%. The difference in refractive index between the air in pores and the cellulose fibers is a primary factor in reducing transparency. The transparency of Film-2 is significantly lower than film-1, due to the interleaving of the longer cellulose fibers leads to the formation of pores in the process of forming Film-2. As the content of CNTs increases, the optical transmittance decreases from 88 to 30%. The opaque CNTs are evenly deposited on the surface of the transparent fiber film, which seriously affects the transparency of the original film. Although FTFHs have a low level of transparency, we could recognize the back pattern of FTFHs.

Figure 3B shows the mechanical properties of Film-1, Film-2, and FTFHs. From **Figure 3B**, we concluded that the tensile strength of film 2 is 32 MPa, similar to that of Film-1 with 30 MPa. The abundant hydrogen groups in regenerated cellulose fiber enhance the contact strength between adjacent regenerated cellulose and improve the tensile strength of the substrate. With the increase of the content of CNTs, the tensile stress of FTFHs will gradually decrease. But, the tensile strength of FTFHs is only slightly lower than that of Film-1, because CNTs would bind with hydrogen bonds of regenerated cellulose fibers and weaken the adhesion between the fibers. The hydrogen bonding can make the CNTs tightly intertwined with the transparent substrate, which can effectively prevent the CNTs from falling off during the use of FTFHs. **Table 2** shows the summary of the mechanical properties of cellulose/CNT composite films and the manufacturing method is the key factor of the mechanical properties of cellulose/CNT composite films.

X-ray Diffraction Profiles of Original Paper and the Regenerated Cellulose

X-ray diffraction (XRD) patterns of the original cellulose and regenerated cellulose are compared in **Figure 4**. The XRD patterns of the original cellulose displayed two distinct characteristic peaks at $2\theta = 14.86$ and $2\theta = 22.75$, which corresponded to the (1–10) and (200) planes of the typical cellulose-I structure, respectively. After the cellulose was dissolved and regenerated, regenerated cellulose showed the typical cellulose II crystalline form, with diffraction peaks at $2\theta = 12.1$ and $2\theta = 21.97$. In the dissolution and regeneration process, cellulose I was transformed into cellulose II, and its crystal structure changed. According to the Segal formula, the crystallinity index (CrI) of original celluloses and regenerated celluloses are 73 and 53%, respectively. The reduced crystallinity demonstrates that the aqueous NMMO solvent enters into the crystallization zone of cellulose and the free hydroxyl groups of cellulose form intramolecular and intermolecular hydrogen bonds with solvent, causing the cellulose to dissolve gradually.

TABLE 2 | Summary of the mechanical properties of cellulose/CNT composite films.

Key materials	Stress (MPa)	Strain (%)	Manufacturing method	Refs.
Original cellulose/CNT	36	2.1	airbrush spraying	Callone et al. (2008)
Original cellulose/CNT	61.6	15.2	casting methond	Xie et al. (2020)
Original cellulose/CNT	180	12	dry–wet spinning	Liang et al. (2022)
Regenerated cellulose/CNT	32	3	Suction filtration	Our work

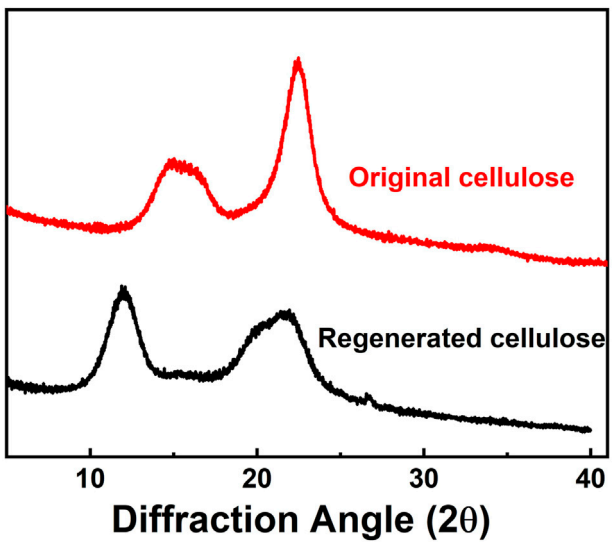

FIGURE 4 | X-ray diffraction profiles of original cellulose and the regenerated cellulose.

Thermal Stability of Original Cellulose and Regenerated Cellulose

The thermal decomposition behavior of original cellulose and regenerated cellulose was investigated by TGA. The results was shown in **Figure 5**. When the temperature rises above 400°C, the residual rate of regenerated cellulose is about 40%, which is about two times of the original cellulose. The glass transition temperature of the regenerated cellulose is 336°C, which is lower the glass transition temperature of original cellulose (361°C). The results of the TGA analysis showed that the thermal stability of the regenerated cellulose is better than original cellulose.

Electrical and Thermal Properties of the Flexible and Transparent Film Heaters

The infrared thermal images of FTFH-0.1, FTFH-0.15, FTFH-0.2 were taken to study their electrical and thermal properties (**Figures 6A–C**). The resistance and generated a temperature of the FTFH-0.1, FTFH-0.15, FTFH-0.2 were shown in **Figure 6D** and **Figure 6E**. All samples were driven at 20 V for 15 s. When the current passes through the FTFH-0.1, FTFH-0.15, FTFH-0.2, they can be rapidly heated from room temperature to 31.8°C, 39.9°C, and 50.5°C and remain stable. The resistance of the FTFH-0.1, FTFH-0.15, FTFH-0.2 is 3423 Ω, 2233 Ω, and 1593 Ω, respectively. The high generated temperature is a significant part of evaluating the performance of the self-heating heater device. As the CNTs' content increases, the resistance of FTFHs' decreases, and the generated temperature rise slowly. It is mainly attributed to the fact that the expansion of CNTs content increases the deposition thickness of CNTs on the flexible film, and the conductive network is formed and improved. However, as the content of CNTs continues to increase, the transparency of FTFHs will be severely affected. In our paper, the content of CNTs is only 0.2 g/m^2, and the generated temperature is as high as 50.5°C. This result demonstrates the feasibility of CNFs deposition on flexible and transparent regenerated cellulose film and FTFHs have broad application prospects in heat preservation heating and electronic devices.

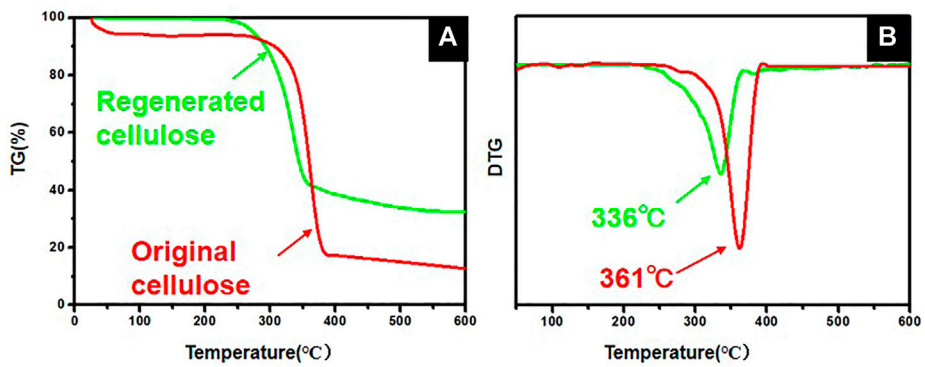

FIGURE 5 | TG and DTG curves of original cellulose and regenerated cellulose. the red lines stand for orginal cellulose, and green lines stand for regenerated cellulose in **Figure 5A,B**.

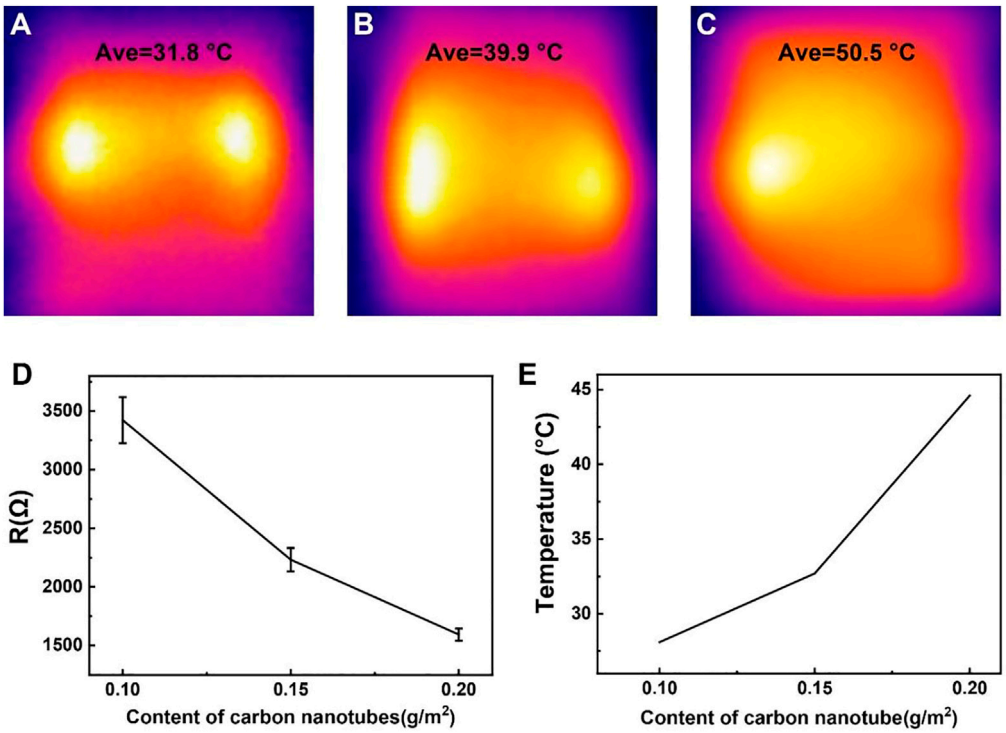

FIGURE 6 | The infrared thermal images: **(A)** FTFH-0.1, **(B)** FTFH-0.15, and **(C)** FTFH-0.2, **(D)** the resistance of FTFH with the content of carbon nanotube ranging from 0.1 g/m^2 to 0.2 g/m^2 **(E)** the generated temperature of the FTFH with the content of carbon nanotubes ranging from 0.1 g/m^2 to 0.2 g/m^2.

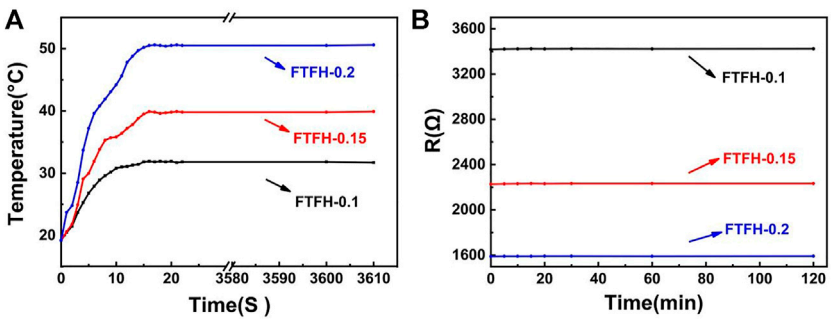

FIGURE 7 | (A) The generated temperature-responsetime of the FTFH with the various carbon nanotubes content. **(B)** The resistance-response time of the FTFH with various carbon nanotubes content.

TABLE 3 | Comparison with other film heaters as previously reported.

Deposition method	Voltage applied (V)	Temp (°C)	Materials	Transparency (%)	Refs.
Chemical techniques	20	90	Carbon fiber composite	70	Lu et al., 2017b
Sputtering	13	100	ITO/CU/ITO films	80	Lee et al., 2020a
PLD	12	140	GZO thin films	85	J Beckford, et al., 2021
Suction filtration	20	40	CNT	90	Our work

Figure 7 exhibits the thermal response time and resistance stability of the FTFHs. As shown in **Figure 7A**, the generated temperature of FTFHs increases with the increase of time, but after 15 s, the generated temperature remained unchanged. This result indicates that FTFHs have a quick thermal response time, and CNTs are an excellent electrothermal material for FTFHs. On

the other hand, the stability of resistance also plays a vital role in FTFHs. The change of the resistance of the FTFHs (**Figure 6B**) along the time was determined, which indicated that the resistance value remains stable and almost no change for about 2 hours. The stability of the resistance is the key to the safety of FTFHs commercial applications. Therefore, the properties of the FTFHs meet the requirement of a flexible and transparent film heater due to shorter response time, the long-term stability of the resistance, and higher generated temperature. **Table 3** exhibits some properties of different film heaters, the two main factors that mainly can affect properties of film heaters are deposition method and materials.

CONCLUSION

In summary, the FTFHs with high optical transmittance, excellent tensile strength, and good heat transfer performance were successfully prepared by simple vacuum filtration. We found that the aqueous NMMO solvent is an excellent solvent system for cellulose, and cellulose that is dissolved and regenerated with aqueous NMMO solution has a small size (0.66 mm in length and 11.45 μm in width). The obtained regenerated cellulose is used to produce flexible transparent film substrates with high optical transparency of 88% (@550 nm) and good mechanical properties of 30 MPa. FTFHs were prepared by depositing CNTs directly on the flexible transparent film, and the extensive hydrogen bonding between CNTs and the cellulose matrix gives FTFHs a high tensile strength of 28 MPa. Furthermore, the FTFHs exhibits higher generation temperatures (50.5°C), shorter response time (15 s), and long-term stability of resistance (2 h). This work demonstrates the broad application prospects of FTFHs in the next generation of green flexible and transparent film heaters.

DATA AVAILABILITY STATEMENT

The original contributions presented in the study are included in the article/supplementary material, further inquiries can be directed to the corresponding author.

AUTHOR CONTRIBUTIONS

Investigation, Visualization, Writing-Original draft preparation; PL: Investigation, Validation, JC and PL contributed this work equally, YL: Formal analysis, Writing-Original draft preparation; KX: Software, YL: Data curation, HS and ZT: Resources, CL: Methodology, DL: Conceptualization, Supervision, Project administration, Funding acquisition, Writing—Review and; Editing.

FUNDING

This work was kindly supported by Guangdong Basic and Applied Basic Research Foundation of Guangdong Province (No. 2020A1515011013; No. 2022A1515010910) and Science and Technology Planning Project of Guangdong Province (No. 2020A050515004) in China.

REFERENCES

Bang, Y. H., Lee, S., Park, J. B., and Cho, H. H. (1999). Effect of Coagulation Conditions on Fine Structure of Regenerated Cellulosic Films Made from cellulose/N-Methylmorpholine-N-oxide/H2O Systems. *J. Appl. Polym. Sci.* 73, 2681–2690. doi:10.1002/(sici)1097-4628(19990923)73:13<2681::aid-app16>3.0.co;2-z

Beckford, J., Behera, M. K., Yarbrough, K., Obasogie, B., Pradhan, S. K., and Bahoura, M. (2021). Gallium Doped Zinc Oxide Thin Films as Transparent Conducting Oxide for Thin-Film Heaters. *AIP Adv.* 11 (7), 075208. doi:10.1063/5.0016367

Callone, E., Fletcher, J. M., Carturan, G., and Raj, R. (2008). A Low-Cost Method for Producing High-Performance Nanocomposite Thin-Films Made from Silica and Cnts on Cellulose Substrates. *J. Mater Sci.* 43 (14), 4862–4869. doi:10.1007/s10853-008-2707-x

Cao, Q., and Rogers, J. A. (2009). Ultrathin Films of Single-Walled Carbon Nanotubes for Electronics and Sensors: A Review of Fundamental and Applied Aspects. *Adv. Mat.* 21, 29–53. doi:10.1002/adfm.20069006510.1002/adma.200801995

Cotterell, B., and Chen, Z. (2004). Buckling and Cracking of Thin Films on Compliant Substrates under Compression. *Int. J. Fract.* 104, 169–179. doi:10.1023/A:1007628800620

De France, K., Zeng, Z., Wu, T., and Nyström, G. (2020). Functional Materials from Nanocellulose: Utilizing Structure-Property Relationships in Bottom-Up Fabrication. *Adv. Mat.* 33, 2000657. doi:10.1002/adma.202000657

De, S., Higgins, T. M., Lyons, P. E., Doherty, E. M., Nirmalraj, P. N., Blau, W. J., et al. (2009). Silver Nanowire Networks as Flexible, Transparent, Conducting Films: Extremely High DC to Optical Conductivity Ratios. *ACS Nano* 3, 1767–1774. doi:10.1021/nn900348c

Fang, Z., Zhu, H., Bao, W., Preston, C., Liu, Z., Dai, J., et al. (2014). Highly Transparent Paper with Tunable Haze for Green Electronics. *Energy Environ. Sci.* 7, 3313–3319. doi:10.1039/c4ee02236j

Gao, X., Li, M., Zhang, H., Tang, X., and Chen, K. (2021). Fabrication of Regenerated Cellulose Films by DMAc Dissolution Using Parenchyma Cells via Low-Temperature Pulping from Yunnan-Endemic Bamboos. *Industrial Crops Prod.* 160, 113116. doi:10.1016/j.indcrop.2020.113116

Guo, B., Zhang, X., Cen, X., Chen, B., Wang, X., Song, M., et al. (2018). Enhanced Mechanical Properties of Aluminum Based Composites Reinforced by Chemically Oxidized Carbon Nanotubes. *Carbon* 139, 459–471. doi:10.1016/j.carbon.2018.07.026

He, C., and Wang, Q. (2000). The Rheological Property of Cellulose Solution in PF/DMSO. *J. China Text. Univ.* 17, 43–46. doi:10.19884/j.1672-5220.2000.03.010

Hutchinson, J. W., and Suo, Z. (1992). Mixed Mode Cracking in Layered materialsAdvances in Applied Mechanics. *Adv. Appl. Mech.* 29, 63–191. doi:10.1016/s0065-2156(08)70164-9

Isogai, A., Saito, T., and Fukuzumi, H. (2011). TEMPO-oxidized Cellulose Nanofibers. *Nanoscale* 3, 71–85. doi:10.1039/c0nr00583e

Isogai, A. (2013). Wood Nanocelluloses: Fundamentals and Applications as New Bio-Based Nanomaterials. *J. Wood Sci.* 59, 449–459. doi:10.1007/s10086-013-1365-z

Jang, J., and Choi, J.-W. (2021). Silver Alloy-Based Metal Matrix Composites: a Potential Material for Reliable Transparent Thin Film Heaters. *J. Mat. Chem. C* 9, 4670–4681. doi:10.1039/D1TC00132A

Ji, Q., Yu, X., Yagoub, A. E.-G. A., Chen, L., and Zhou, C. (2021). Efficient Cleavage of Strong Hydrogen Bonds in Sugarcane Bagasse by Ternary

Acidic Deep Eutectic Solvent and Ultrasonication to Facile Fabrication of Cellulose Nanofibers. *Cellulose* 28, 6159–6182. doi:10.1007/s10570-021-03876-w

Khakalo, A., Filpponen, I., and Rojas, O. J. (2017). Protein Adsorption Tailors the Surface Energies and Compatibility between Polylactide and Cellulose Nanofibrils. *Biomacromolecules* 18, 1426–1433. doi:10.1021/acs.biomac.7b00173

Kim, Y. H., Sachse, C., Machala, M. L., May, C., Müller-Meskamp, L., and Leo, K. (2011). Highly Conductive PEDOT:PSS Electrode with Optimized Solvent and Thermal Post-Treatment for ITO-free Organic Solar Cells. *Adv. Funct. Mat.* 21, 1076–1081. doi:10.1002/adfm.201002290

Kong, W., Yu, G., Xing, J., Zhang, H., Liu, M., and Shi, Y. (2021). Effect of the Dissolving Method on the Dissolution of Dissolving Pulp Cellulose Fibers with Different Dried-States in Different NaOH/Additives Aqueous Solutions. *J. Polym. Environ.* 29, 3909–3917. doi:10.1007/s10924-021-02149-8

Lee, E. Y., Han, K., Kim, D. H., Park, Y.-M., Kwon, H.-S., Yoon, K.-H., et al. (2020a). Exposure-weighted Scoring for Metabolic Syndrome and the Risk of Myocardial Infarction and Stroke: a Nationwide Population-Based Study. *Cardiovasc. Diabetol.* 19 (1), 153. doi:10.1186/s12933-020-01129-x

Lee, H., Kim, M., KimLee, I. H., and Lee, H. (2016). Flexible and Stretchable Optoelectronic Devices Using Silver Nanowires and Graphene. *Adv. Mat.* 28, 4541–4548. doi:10.1039/C4TC02448F10.1002/adma.201505559

Lee, S., Jang, J., ParkParkChung, T. Y. M. C. H., Park, Y. M., Park, J. S., Kim, Y.-K., et al. (2020b). Electrodeposited Silver Nanowire Transparent Conducting Electrodes for Thin-Film Solar Cells. *ACS Appl. Mat. Interfaces* 12, 6169–6175. doi:10.1021/acsami.9b17168

Li, Z., Liu, W., Guan, F., Li, G., Song, Z., Yu, D., et al. (2019). Using Cellulose Fibers to Fabricate Transparent Paper by Microfibrillation. *Carbohydr. Polym.* 214, 26–33. doi:10.1016/j.carbpol.2019.03.019

Liang, Q., Zhang, D., Wu, Y., Chen, S., Han, Z., Wang, B., et al. (2022). Self-Stretchable Fiber Liquid Sensors Made with Bacterial Cellulose/Carbon Nanotubes for Smart Diapers. *ACS Appl. Mat.* 18, 21319–21329. doi:10.1021/acsami.2c00960

Lu, P., Cheng, F., Ou, Y., Lin, M., Su, L., Chen, S., et al. (2017b). A Flexible and Transparent Thin Film Heater Based on a Carbon Fiber /heat-Resistant Cellulose Composite. *Compos. Sci. Technol.* 153, 1–6. doi:10.1016/j.compscitech.2017.09.033

Lu, P., Cheng, F., Ou, Y., Lin, M., Su, L., Chen, S., et al. (2017a). Rapid Fabrication of Transparent Film Directly from Wood Fibers with Microwave-Assisted Ionic Liquids Technology. *Carbohydr. Polym.* 174, 330–336. doi:10.1016/j.carbpol.2017.06.057

Ma, H., Yu, J., Liu, L., and Fan, Y. (2021). An Optimized Preparation of Nanofiber Hydrogels Derived from Natural Carbohydrate Polymers and Their Drug Release Capacity under Different pH Surroundings. *Carbohydr. Polym.* 265, 118008. doi:10.1016/j.carbpol.2021.118008

Madaria, A. R., Kumar, A., and Zhou, C. (2011). Large Scale, Highly Conductive and Patterned Transparent Films of Silver Nanowires on Arbitrary Substrates and Their Application in Touch Screens. *Nanotechnology* 22, 245201. doi:10.1088/0957-4484/22/24/245201

Protz, R., Lehmann, A., Ganster, J., and Fink, H.-P. (2021). Solubility and Spinnability of Cellulose-Lignin Blends in Aqueous NMMO. *Carbohydr. Polym.* 251, 117027. doi:10.1016/j.carbpol.2020.117027

Sayyed, A. J., Mohite, L. V., Deshmukh, N. A., and Pinjari, D. V. (2019). Structural Characterization of Cellulose Pulp in Aqueous NMMO Solution under the Process Conditions of Lyocell Slurry. *Carbohydr. Polym.* 206, 220–228. doi:10.1016/j.carbpol.2018.11.004

Song, C., Zhang, N., Lin, J., Guo, X., and Liu, X. (2017). Sb2O3/Ag/Sb2O3 Multilayer Transparent Conducting Films for Ultraviolet Organic Light-Emitting Diode. *Sci. Rep.* 7, 1–7. doi:10.1038/srep41250

Su, L., Ou, Y., Feng, X., Lin, M., Li, J., Liu, D., et al. (2019). Integrated Production of Cellulose Nanofibers and Sodium Carboxymethylcellulose through Controllable Eco-Carboxymethylation under Mild Conditions. *ACS Sustain. Chem. Eng.* 7, 3792–3800. doi:10.1021/acssuschemeng.8b04492

Tokuno, T., Nogi, M., Karakawa, M., Jiu, J., Nge, T. T., Aso, Y., et al. (2011). Fabrication of Silver Nanowire Transparent Electrodes at Room Temperature. *Nano Res.* 4, 1215–1222. doi:10.27200/d.cnki.gkmlu.2019.00191910.1007/s12274-011-0172-3

Wang, J., Jiu, J., Zhang, S., Sugahara, T., Nagao, S., Suganuma, K., et al. (2018). The Comprehensive Effects of Visible Light Irradiation on Silver Nanowire Transparent Electrode. *Nanotechnology* 29, 435701. doi:10.1088/1361-6528/aad619

Xie, Y., Xu, H., He, X., Hu, Y., Zhu, E., Gao, Y., et al. (2020). Flexible Electronic Skin Sensor Based on Regenerated Cellulose/carbon Nanotube Composite Films. *Cellulose* 27 (14), 10199–10211. doi:10.1007/s10570-020-03496-w

Yu, H., Fang, D., Dirican, M., Wang, R., Tian, Y., Chen, L., et al. (2019). Binding Conductive Ink Initiatively and Strongly: Transparent and Thermally Stable Cellulose Nanopaper as a Promising Substrate for Flexible Electronics. *ACS Appl. Mat. Interfaces* 11, 20281–20290. doi:10.1021/acsami.9b04596

Yu, S., Liu, X., Wu, M., Dong, H., Wang, X., and Li, L. (2021). All-Solution-Processed Molybdenum Oxide-Encapsulated Silver Nanowire Flexible Transparent Conductors with Improved Conductivity and Adhesion. *ACS Appl. Mat. Interfaces* 13, 14470–14478. doi:10.1021/acsami.0c22324

Zhang, D., Ryu, K., Liu, X., Polikarpov, E., Ly, J., Tompson, M. E., et al. (2006). Transparent, Conductive, and Flexible Carbon Nanotube Films and Their Application in Organic Light-Emitting Diodes. *Nano Lett.* 6, 1880–1886. doi:10.1021/nl0608543

Zhang, Q., Wang, A., Zhang, S., Li, N., Chen, S., Zhang, Y., et al. (2017a). Asymptomatic Polyvascular Disease and the Risks of Cardiovascular Events and All-Cause Death. *Atherosclerosis* 262, 1–7. doi:10.1016/j.atherosclerosis.2017.04.015

Zhang, Y., Tang, S., and Zhang, T. (2017b). Homogeneous Alkalization of Cellulose in N-Methylmorpholine-N-Oxide/water Solution. *Cellulose* 24, 1235–1245. doi:10.1007/s10570-017-1195-z

Zimmermann, R., Müller, Y., Freudenberg, U., Jehnichen, D., Potthast, A., Rosenau, T., et al. (2016). Oxidation and Structural Changes in NMMO-Regenerated Cellulose Films. *Cellulose* 23, 3535–3541. doi:10.1007/s10570-016-1084-x

Conflict of Interest: PL, TZ was employed by Gree Intelligent Equipment Co., Ltd.

The remaining authors declare that the research was conducted in the absence of any commercial or financial relationships that could be construed as a potential conflict of interest.

Publisher's Note: All claims expressed in this article are solely those of the authors and do not necessarily represent those of their affiliated organizations, or those of the publisher, the editors and the reviewers. Any product that may be evaluated in this article, or claim that may be made by its manufacturer, is not guaranteed or endorsed by the publisher.